Journal of Power Sources 192 (2009) 258–266

Contents lists available at ScienceDirect

Journal of Power Sources

journal homepage: www.elsevier.com/locate/jpowsour

Membrane electrode assemblies for high-temperature polymer electrolyte fuel cells based on *poly*(2,5-benzimidazole) membranes with phosphoric acid impregnation via the catalyst layers

Christoph Wannek*, Werner Lehnert, Jürgen Mergel

Institute of Energy Research – Fuel Cells (IEF-3), Forschungszentrum Jülich GmbH, 52425 Jülich, Germany

ARTICLE INFO

Article history:
Received 23 November 2008
Received in revised form 8 March 2009
Accepted 23 March 2009
Available online 2 April 2009

Keywords:
Acid doping
Catalyst layer
High-temperature polymer electrolyte fuel cell
Membrane electrode assembly
poly(2,5-Benzimidazole)
Phosphoric acid

ABSTRACT

A novel strategy for introducing phosphoric acid as the electrolyte into high-temperature polymer electrolyte fuel cells by using acid impregnated catalyst layers instead of pre-doped membranes is presented in this paper. This experimental approach is used for the development of membrane electrode assemblies based on *poly*(2,5-benzimidazole) (ABPBI) as the membrane polymer. The acid uptake of free-standing ABPBI used for this work amounts to ABPBI × 3.1 H_3PO_4 which has a specific conductivity of ~80 mS cm^{-1} at 140 °C. Rather thick catalyst layers (20% Pt/C, 1 mg Pt cm^{-2}, 40% PTFE as binder, d = 100–150 μm) are prepared on gas diffusion layers with a dense hydrophobic microlayer. After impregnation of the catalyst layers with phosphoric acid and assembling them with a mechanically robust undoped ABPBI membrane a fast redistribution of the electrolyte occurs during cell start-up. Power densities of about 250 mW cm^{-2} are achieved at 160 °C and ambient pressure with hydrogen and air as reactants. Details of membrane properties, preparation and optimization of gas diffusion electrodes and fuel cell characterization are discussed. We consider our novel approach to be especially suitable for an easy and reproducible fabrication of MEAs with large active areas.

1. Introduction

Polymer electrolyte fuel cells (PEFCs) with working temperatures significantly higher than 100 °C do not require high-purity hydrogen as fuel, and therefore they are beneficial for devices that run on hydrogen produced on site by the reforming of hydrocarbon energy carriers. In fact, high-temperature PEFCs (HT-PEFCs) operating at 160–200 °C 'tolerate' the 1 or 2% of carbon monoxide contained in fuel gases produced by autothermal or steam reforming after the so-called shift reaction, while for a classical PEFC running at 80 °C the CO content has to be reduced by additional reactors to levels around or below 50 ppm [1]. Facilitated dissipation of waste heat due to a large temperature difference from the environment (and thus the use of comparatively small radiators) and the fact that HT-PEFCs are not reliant on intricate water management (because the water needed in the electrolyte in classical PEFCs is replaced by non-volatile phosphoric acid) represent further advantages of this special type of fuel cell, making the fuel processing and ancillary system comparatively small and simple, which is beneficial for the overall efficiency of the fuel cell system. Fuel cell auxiliary power units (APUs) running on reformed diesel or kerosene could supply vehicles such as trucks, locomotives or aircraft with electrical power at much higher energy efficiency when these vehicles are not in motion than can be achieved by idling of the main engine. Combined heat and power applications running on reformed methane (>85% overall efficiency – electricity plus heat – achievable [2]) are another favourable application of this special type of PEFCs.

The only technically viable and relevant HT-PEFCs operating at 160–200 °C that are under development today rely on proton transport in phosphoric acid which is fixed to a polybenzimidazole type membrane. While most of the development in recent years has been focused on membrane electrode assemblies (MEAs) based on *poly*(2,2′-(*m*-phenylene)-5,5′-bibenzimidazole) (PBI; Fig. 1, top) and its blends [3–17], the use of the alternative chemically related membrane polymer *poly*(2,5-benzimidazole) (ABPBI; Fig. 1, bottom) is emerging [18–23].

In the open literature, several pathways for introducing the phosphoric acid needed for the proton conductivity of the membrane have been developed and described. The classical approach consists of doping free-standing sheets of the benzimidazole type membrane in concentrated phosphoric acid [3–6,12–21]. In this method, membranes with acid contents of up to 70–80 wt.% (e.g. corresponding to a chemical formula PBI × 8–12 H_3PO_4) are obtained [5]. However, due to the large uptake of liquid acid these membranes display significant dimensional swelling, which may

* Corresponding author. Tel.: +49 2461 614013; fax: +49 2461 616695.
E-mail address: c.wannek@fz-juelich.de (C. Wannek).

0378-7753/$ – see front matter © 2009 Elsevier B.V. All rights reserved.
doi:10.1016/j.jpowsour.2009.03.051

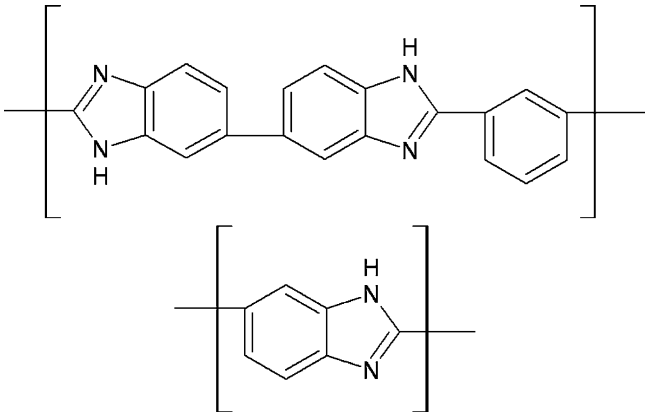

Fig. 1. Structures of the repeating units of PBI (= *poly*(2,2′-(*m*-phenylene)-5,5′-bibenzimidazole) – left) and ABPBI (= *poly*(2,5-benzimidazole) – right).

not always be homogeneous in all spatial directions and, more importantly, the mechanical properties of these membranes may become critically poor, making the reproducible production of MEAs for cells with a large active area challenging. As a consequence, moderate doping levels have been preferred for the assembly of MEAs [6,16–21]. A second, very elegant way of fabricating this type of electrolyte yielding PBI membranes with an even higher content of phosphoric acid and thus showing very high conductivity is characterized by solution polymerization of the monomers in polyphosphoric acid (PPA) followed by membrane formation as a consequence of controlled hydrolysis of the polyphosphoric acid to orthophosphoric acid [7,9]. However, this procedure is not applicable in the case of membrane polymers such as ABPBI which – before performing a cross-linking step after membrane formation – are soluble in phosphoric acid. A third pathway consists of preparing a 'dry' catalyst-coated PBI membrane and contacting it with gas diffusion layers (GDLs) which are loaded with appropriate amounts of H_3PO_4 during MEA assembly [11]. The published fuel cell performance data show that a transfer of phosphoric acid from the rather hydrophobic GDLs into the membrane occurs easily. Nevertheless, in this type of MEAs it appears to be difficult or perhaps even impossible to use microporous layers (ML) as barrier layers between the membrane and electrodes on the one side and the GDL substrate on the other side to minimize the leaching of phosphoric acid from the electrolyte as the phosphoric acid would have to cross this barrier during the cell start-up process.

A fourth pathway, acid impregnation of the MEA via the catalyst layers, was identified at a very early point [24] but was not pursued systematically in academic research in the past and has only been referred to in a few patent applications (e.g. [25,26]). In the following, we show how MEAs with good fuel cell performance due to high conductivity of the electrolyte that show very good durability (implying little acid leaching) can be easily and reproducibly prepared by assembling undoped ABPBI membranes with gas diffusion electrodes based on GDLs (with microporous layers) in which the catalyst layers are loaded with phosphoric acid. We present the results of our studies on the influences of various parameters concerning the composition of the catalyst layers, their noble metal loading as well as the amount of acid impregnation on the fuel cell performance of so-prepared HT-PEFCs. Characterization was carried out with pure hydrogen and air as the reactants at $T = 160\,^{\circ}C$ and ambient pressure during the first 200 h of service. Other features such as the influence of some fuel cell operation parameters [22], studies of the durability of fuel cell performance [23] or first results about the spatially resolved acid distribution in the MEAs [27] have been presented elsewhere.

2. Experimental

The ABPBI (= *poly*(2,5-benzimidazole)) membranes used for this study were supplied by FuMA-Tech in 2006. They were obtained in an acid-free form with a thickness of 27 (±3) μm. These membranes with a relatively high degree of chemical cross-linking represent a compromise between high acid uptake (and thus high conductivity) and sufficient mechanical stability during prolonged fuel cell operation including temperature and load cycles [28].

2.1. Preparation of gas diffusion electrodes impregnated with phosphoric acid

For the fabrication of gas diffusion electrodes (GDEs), slurries containing appropriate amounts of platinum catalysts (either supported on carbon or Pt black) with precious metal weight fractions from 20 to 100 wt.% (HiSPEC 3.000, 4.000, 9.000 and 1.000 from Johnson Matthey) and aqueous dispersions of PTFE (Dyneon) were prepared by ultrasonic agitation for 20–40 min in a mixture of water and organic alcohols. These inks were coated onto the microporous layer of a commercially available woven GDL (HT 1400-W from E-TEK, a division of BASF Fuel Cell Inc.) by an automated doctor blade technique followed by a drying step. The platinum loadings of all GDEs used for this study were between 0.8 and 1.2 mg cm^{-2}, unless otherwise stated. A short discussion about the preparation of GDEs containing ABPBI in the catalyst layer is given separately in Section 3.4.3.

Impregnation of the catalyst layers with predefined amounts of phosphoric acid was carried out by pipetting a mixture of H_3PO_4 and ethanol (1:5 by volume) onto the top of the GDEs in three stages at intervals of 60 min. Afterwards the ethanol was allowed to evaporate overnight.

2.2. Physico-chemical analyses

2.2.1. Water and acid uptake measurements

The membranes were dried at 100 °C for 1 h prior to the water and acid uptake tests. After measuring the lengths and weights of dry sheets with areas of about 25 cm^2 they were immersed in aqueous phosphoric acid of different concentrations for 8 h at 80 °C. The sum of the water and acid uptake was determined by weighing the membranes after removing the liquid from the membrane surfaces by blotting with a paper towel. Afterwards the samples were dried at 100 °C in an oven to constant weight. We assume that during this step the water absorbed during the soaking process evaporated while the phosphoric acid remained in the membrane.

2.2.2. Membrane conductivity

The proton conductivity of acid-doped ABPBI membranes was determined by means of an in-plane four-point technique in a custom-designed test rig constructed at our institute (Fig. 2). To ensure good contact between the sample and all four electrodes, the membrane was threaded between the four platinum electrodes (from left to right above – below – above – below the membrane) of the test cell, which was situated inside a glass container kept in a conventional laboratory oven in order to regulate the temperature of the sample. The water vapour pressure around the membrane during the measurement was regulated by adjusting the dew point of the air which was blown constantly at moderate flow rates through the glass container. The temperature and relative humidity in the vicinity of the sample were measured with a dew point sensor.

The specific conductivity σ was calculated using the equation $\sigma = l/(Rdw)$, where l is the distance between the inner electrodes, d and w are the thickness and the width of the acid-doped membrane, respectively, and R is the resistance obtained from AC impedance

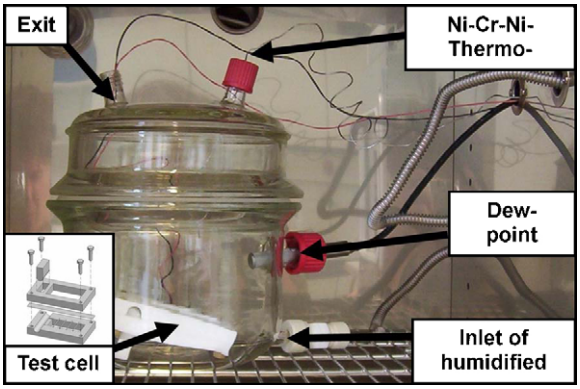

Fig. 2. Photo of the home-built set-up for the determination of membrane conductivities at different temperatures ($RT \leq T \leq 180\,^{\circ}C$) and relative humidities ($8\,^{\circ}C \leq T_d \leq 95\,^{\circ}C$).

spectroscopy over a frequency range of 500 Hz to 65 kHz with an oscillating voltage of 20 mV by using the low intersect of the high-frequency semicircle with the 'real' axis in the complex impedance plane.

For the calculation of the specific conductivity we used the values of thickness and width of the sample before the first heating during the conductivity measurement. Prior to the measurements, the samples were conditioned by maintaining them in the test cell at the respective temperature and humidity for at least 30 min.

2.2.3. Rheology

The rheological behaviour of the catalyst inks was measured with a rotational rheometer in plate/plate geometry (Rheo Stress 1, Haake) using controlled shear stress tests. The viscosities of the catalyst inks at shear rates between 10 and 50 s^{-1} were used to compare the properties of different dispersions, as these shear rates are close to the conditions during the bar-coating of the catalyst inks onto the GDLs.

2.2.4. Dynamic light scattering

The stability of different catalyst inks and the particle size distribution in them was determined by photon cross-correlation spectroscopy (PCCS; measuring instrument: Nanophox, Sympatec GmbH). Although with this special dynamic light-scattering technique the use of two laser beams is intended to allow the characterization of turbid and opaque dispersions, the catalyst inks had to be diluted with the same mixture of water and alcohols used for their preparation until the solids content was below 0.1% by volume. Each sample was characterized by performing 10 measurements in series (each of them taking 30–50 min) to gain information about agglomeration and/or sedimentation processes. The particle size distributions were deduced from the slopes of the individual cross correlation functions via a non-negative least squares fit.

2.2.5. Scanning electron microscopy

The microstructure of the fabricated gas diffusion electrodes was studied with a scanning electron microscope (Zeiss Supra50). The samples were sputtered with a thin layer of platinum prior to characterization. To minimize the impact of the electron beam on the polymer phase (PTFE) in the catalyst layers, images were taken with a low accelerating voltage of only 2 keV.

2.3. MEA assembly and fuel cell characterization

The MEAs were assembled by contacting GDEs impregnated with phosphoric acid with undoped sheets of ABPBI membrane in the test cells without a preceding hot-pressing step. Together with gaskets made of fluorinated polymer, the MEAs with an active area of 14.4 cm^2 were compressed to a constant gap (in most cases to 75% of the sum of the thicknesses of the individual components) between graphitic (BBP4, SGL Carbon) triple serpentine flow fields and solid metallic endplates equipped with heating cartridges. The cell performances were studied at ambient pressure using pure hydrogen and air as reactants. For all experiments, the mass flows of the reactants for current densities equal to or greater than 200 mA cm^{-2} were adjusted to predefined values of the stoichiometric excesses λ. At lower current densities, the gas flows were fixed to the respective values for $j = 200$ mA cm^{-2}. Unless otherwise stated, the characterization was performed with $\lambda_{anode/cathode} = 2/2$.

Polarization curves were recorded by first increasing the current density stepwise from open circuit voltage (OCV) until the cell voltage dropped below a predefined value (mostly 350 mV), and subsequently lowering it with the same step size back to OCV. At each current density, after a hold time of 30 s the cell voltage was measured every 9 s and the average of four data points was calculated. To draw the polarization curves, the data measured at the respective current densities during the 'round-trip' (OCV ⇒ <350 mV ⇒ OCV) were averaged. The differences between the two values were always smaller than 30 mV for OCV and smaller than 10 mV at all current densities. When no polarization curves were measured the cells were run at constant current densities, which resulted in cell voltages of about 600 mV (in most cases $j = 200$ mA cm^{-2}). Cell resistances were measured by the current interruption technique.

3. Results and discussion

3.1. Water and phosphoric acid uptake of ABPBI

Like other polybenzimidazoles ABPBI readily absorbs large amounts of water and especially phosphoric acid while no uptake of most organic solvents is observed. Even when immersed in strong dipolar and non-protogenic solvents such as dimethylsulfoxide (DMSO), N-methylpyrrolidone (NMP) or dimethylacetamide (DMAc), the cross-linked ABPBI membranes showed no or very little swelling. The water and acid uptake of ABPBI membranes caused by doping in aqueous phosphoric acid of different concentrations at 80 °C is depicted in Fig. 3. The weight gain in pure water corresponds to about one water molecule per repeat unit of polymer (i.e. an acid–base reaction with each nitrogen atom). With increasing H_3PO_4 concentration of the doping bath the phosphoric acid uptake increases strongly. To a smaller extent, the water uptake also rises. For example, the composition of membranes doped in

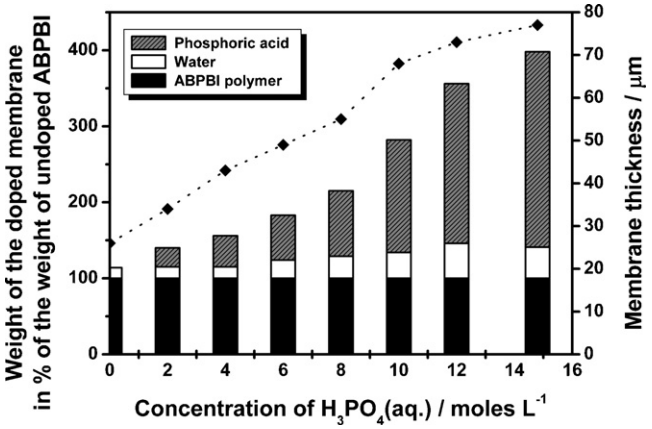

Fig. 3. Water and phosphoric acid uptake of ABPBI membranes during immersion in aqueous phosphoric acid of different concentrations for eight hours at 80 °C (left axis), the thickness of the membranes after doping is shown on the right axis.

2 M H_3PO_4 corresponds to ABPBI × 0.3 H_3PO_4 whereas dipping the membrane in a bath with 8 mol L^{-1} phosphoric acid resulted in ABPBI × 1.0 H_3PO_4. After doping in 85% (or 14.8 M) phosphoric acid, the membrane weight was quadrupled and the membrane contained as many as 3.1 molecules of phosphoric acid per repeat unit. For ABPBI with a lower degree of cross-linking slightly higher doping levels have been reported recently (ABPBI × 3.5 H_3PO_4 [22,23]). With an acid content of about 72% in the water-free membrane, the doping level of the present material is as high as observed for classical PBI membranes [5] but still significantly lower than reported for PBI membranes produced by the sol–gel reaction from polyphosphoric acid [7,9,10]. We observed that the swelling was strongly anisotropic as the lateral dimensions of the samples increased by less than 4% while the thickness almost tripled during doping in concentrated phosphoric acid. As a rough estimate, we observed that more than half of the acid uptake of the membranes occurred during the first 10 min of the doping process at 80 °C and more than 90% during the first hour.

3.2. Proton conductivity of phosphoric-acid-doped ABPBI membranes

Although for the present study the concept of cell assembly from undoped membranes and acid-impregnated gas diffusion electrodes was pursued, the conductivity of free-standing ABPBI × 3.1 H_3PO_4 was measured at different temperatures and relative humidities to gain information about the membrane conductivities which might be achieved in the operating fuel cell after redistribution of the phosphoric acid within the MEA.

The specific conductivity of ABPBI doped in concentrated phosphoric acid measured under 'dry' conditions in our test rig shows S-shaped behaviour depending on the cell temperature (Fig. 4). The increase of proton conductivity with temperature between 100 and 140 °C is due to growing proton mobility in the membrane [4]. At 140 °C the specific conductivity amounts to 79 mS cm^{-1}, which confirms the data previously reported for ABPBI × 3.5 H_3PO_4 [22,23]. This value is higher than that published earlier for ABPBI by other research groups [19,20] and is also in the same order of magnitude as that reported for PBI doped in concentrated phosphoric acid [4,5,12,13,17]. The conductivity of PBI manufactured via the sol–gel process from PPA has been reported to be even higher [7,9]. The flattening of the curve above 150 °C can be attributed to the (reversible) condensation of phosphoric acid (H_3PO_4) to pyrophosphoric acid ($H_4P_2O_7$), which has been reported to have a lower conductivity than H_3PO_4 [4,12]. At low temperatures, we measured abnormally

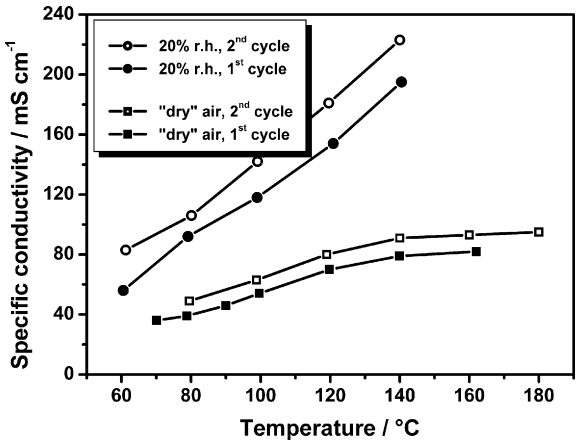

Fig. 4. Specific conductivity of ABPBI × 3.1 H_3PO_4 at different temperatures and water vapour pressures. Values were calculated on the basis of the thickness of the acid-containing membrane before the first heating.

Table 1
Composition and thickness of catalyst layers (difference of thicknesses of GDL and GDE as measured with a micrometer with a clamping pressure of 160 kPa) with a platinum loading of 1 mg cm^{-1} based on different types of catalysts and their visual appearance after impregnation with 20 mg H_3PO_4 cm^{-2}.

Catalyst	PTFE content	Catalyst layer thickness (μm)	Visual appearance of the GDEs in the acid-loaded state
Pt black	10%	10	Liquid film of H_3PO_4 on the surface
60% Pt/C	24%	25	Puddles of H_3PO_4 on the surface
40% Pt/C	32%	50	No droplets on the top, slightly shiny
20% Pt/C	40%	150	Dry

high specific conductivities due to the fact that in our test rig the air around the sample had been bubbled though a water bath at room temperature followed by being passing through a combination of a Liebig and Dimroth condenser connected to a refrigerated circulator bath. With this set-up, the atmosphere around the sample always contains water with a dew point of about 8–10 °C, which is of little importance to the conductivity at high temperature as the relative humidities are well below 1%. Nevertheless, with decreasing temperature the measurements were no longer conducted under nearly dry conditions but at significant humidity levels of, for example 4% at 70 °C, leading to higher specific conductivity [3–5,13,19].

We decided to use the data obtained from the first heating of the samples. In the second run we always measured much higher conductivities (Fig. 4). We relate this phenomenon to the observation that at high temperatures the samples started to 'sweat out' some liquid which did not re-enter the membrane during the cooling step. We speculate that this liquid acid might lead to some surface conductivity influencing the result of the second circle.

Much higher conductivities were measured at a constant relative humidity of 20% reaching nearly 200 mS cm^{-1} at 140 °C (dew point of 90 °C!) during the first cycle. This is in accordance with the fact that the conductivity of the binary mixture of phosphoric acid and water has a maximum at an intermediate composition (e.g. at ~50% H_3PO_4 at RT [5]) as well as with previous reports on the properties of acid-containing membranes of the polybenzimidazole type [3–5,13,19].

In the operating fuel cell, the effective membrane conductivity depends on a complicated equilibrium between the properties of the free-standing membrane, the compression of the MEA in the cell, the humidity of the fuel steam (hydrogen or technical reformate) and the amount of product water produced by the cell.

3.3. Catalyst inks, microstructure of the catalyst layer and reflections about the re-distribution of H_3PO_4 in the MEA

Ultrasonication for at least 20 min turned out to be necessary to reproducibly prepare homogeneous catalyst inks containing black or carbon-supported platinum catalyst and PTFE in a mixture of water and alcohols. Dynamic light scattering analyses performed on the (diluted) dispersions revealed that small average 'particle sizes' of less than 1 μm and very narrow particle size distributions were obtained for all combinations of catalysts and PTFE concentrations listed in Table 1. The representative example depicted in Fig. 5 containing the data for the combination of 20% Pt/C and 40% PTFE in the dry catalyst layer shows that the mean diameter of the individual particles (assumed to be spherical) was calculated as about 250 nm. This 'particle size' corresponds to the 'aggregate structure' of carbon black characterized by several individual (more or less spherical) primary carbon particles being joined or fused together to form rod-like structures with some branching [29]. This type

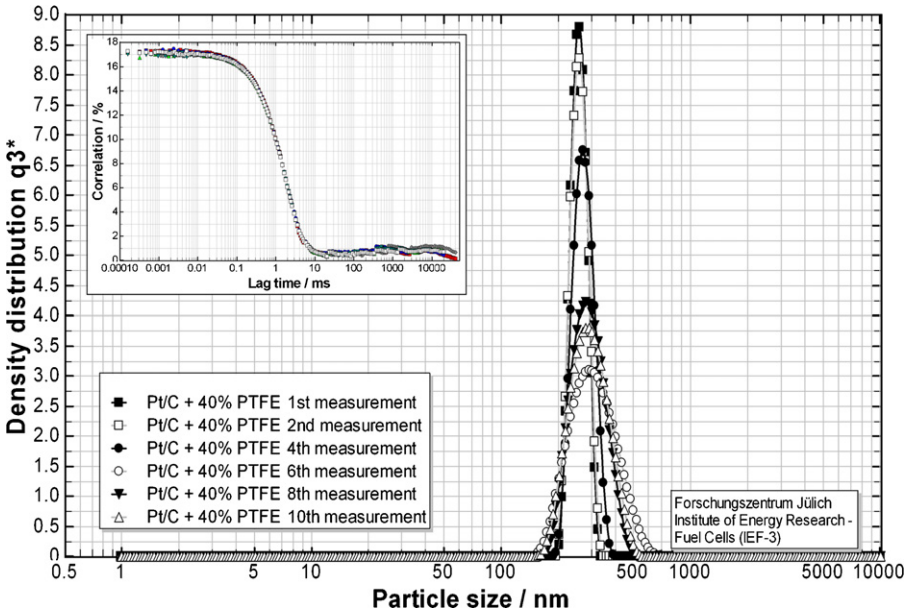

Fig. 5. Development of the correlation function of a (diluted) catalyst ink containing 20% Pt/C and 40% PTFE (solids content; small inset) and the particle size distribution deduced from this data by non-negative least-square fitting over a measuring time of 8 h.

of aggregate structure is commonly observed during TEM experiments performed on fuel cell catalysts (see for example [30]). These results indicate that the application of energy to the catalyst ink by ultrasonic agitation leads to dispersion of the catalyst in form of fine particles with diameters smaller than 1 μm without destroying the aggregate structure of carbon black. No significant changes in the correlation functions (small inset in Fig. 5) between the first and the tenth measurement (performed at an interval of more than 7 h) are visible. The particle size distribution deduced from this data shows only a slight broadening and increase of the mean particle size.

The microstructure of the dried catalyst layers was checked by optical and scanning electron microscopy. While the thin electrodes prepared with Pt black and 60% Pt/C hardly had any cracks on their surface, the much thicker catalyst layers containing 40% Pt/C, and especially the one prepared with 20% Pt/C, consisted of many individual clots of 1–3 mm in diameter with sharp edges (Fig. 6a). A homogeneous distribution of PTFE was achieved in all samples listed in Table 1. As can be seen from Fig. 6b, there is no phase separation between the catalyst particles and polymer on the scale from micro- to millimetres even in the sample with 20% Pt/C containing 40 wt.% PTFE. The high-resolution image of the same sample shows how the individual carbon particles of the catalyst are connected by a web of very thin polymer strings. Only when the PTFE content in the catalyst layer exceeds a given value does it become impossible for all of the polymer to be distributed homogeneously under the preparation conditions used for this study (cf. Fig. 6d). The results of our efforts to prepare catalyst layers containing the membrane polymer ABPBI are discussed separately in Section 3.4.3.

After the acid-impregnated GDEs had been assembled with the undoped membrane in the cell and a leak test under nitrogen had been performed, the samples were heated up to 160 °C under OCV conditions with hydrogen and air flowing through the anodic and cathodic compartments. The cell voltage increased steadily during the beginning of the heating process, reached about 1.0 V at 60–80 °C and then decreased slightly to 850–950 mV at 160 °C. Before starting to draw current the cell was maintained at OCV for 60 min to provide sufficient time for the phosphoric acid to be re-distributed in the MEA, and thus to achieve good proton conductivity of the membrane. Afterwards the current density was increased stepwise within 30 min to $j = 200\ \mathrm{mA\,cm^{-2}}$ resulting in a cell voltage of about 600 mV. During a following 70–100 h hold step at this current density the cell voltage changed only marginally. From these observations we conclude that acid redistribution within the MEA, and especially the transfer of phosphoric acid from the catalyst layers into the membrane at 160 °C, is a rather quick process with an equilibrium being established within less than 1 h.

3.4. Influence of the composition of the catalyst layer and the fuel cell operating conditions on MEA performance

3.4.1. Choice of platinum catalyst

Gas diffusion electrodes with a platinum loading of $1\ \mathrm{mg\,cm^{-2}}$ were prepared with four types of catalysts ranging from 20% Pt/C to platinum black. For these experiments the amount of PTFE binder in the catalyst layers was adjusted to the carbon contents of the different catalyst layers guided by the information from [31] without further optimization (Table 1). As has been shown above, the H_3PO_4 uptake of the ABPBI membrane in concentrated phosphoric acid amounts to 50 μm (Fig. 3), which corresponds to $10.5–11.0\ \mathrm{mg\,cm^{-2}}$. As a consequence, both the anode and cathode must be loaded with at least half of this quantity – further below we will show that a considerable excess is actually necessary – to assure good performance of MEAs with acid impregnation via the electrodes, i.e. an amount of $>5.5\ \mathrm{mg\,H_3PO_4\,cm^{-2}}$ or the equivalent of a dense film of phosphoric acid more than 25 μm thick has to be stored in each of the catalyst layers before the MEA can be assembled. Furthermore, taking into account that their porosity might be ~60% [6] we conclude that catalyst layers suitable for this MEA preparation technique have to be significantly thicker than 50 μm. This consideration is corroborated by the observation that the GDEs based on Pt black and 60% Pt/C were not able to store the complete amount of acid necessary for good MEA performance ($20\ \mathrm{mg\,cm^{-2}}$, Table 1) as they were simply too thin. The GDE based on 40% Pt/C took up the entire amount of acid, but it was shining wet as if completely soaked with acid. In this context, it is worth mentioning that MEAs with this type of GDE needed high cathodic air flows (up to $\lambda = 6$) to give reasonable fuel cell performance. Only the very thick electrodes based on 20% Pt/C stored the complete amount of phosphoric acid without any problems and maintained a dry appearance. As a consequence, all the experiments described and

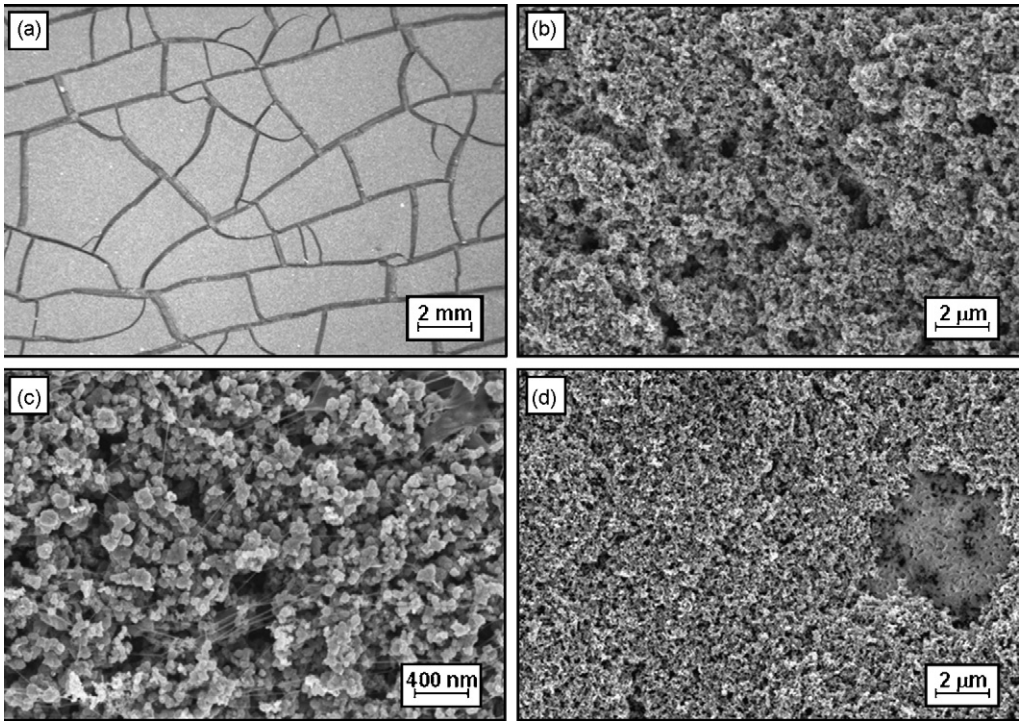

Fig. 6. Images of the microstructure of catalyst layers based on 20% Pt/C taken with an optical microscope (a) and a scanning electron microscope (b–d), respectively. Figures (a–c) present different magnifications of the surface of a catalyst layer with 40 wt.% PTFE. The sample depicted in (d) contains 50% PTFE; as described in detail in the main text (Section 3.4.2) on the right hand side a PTFE agglomerate is clearly discernible.

discussed in the following were performed with this type of thick GDE based on 20% Pt/C.

3.4.2. Optimization of PTFE content in catalyst layer

We studied the influence of the PTFE content within the catalyst layer based on 20% Pt/C within the range of 20–60 wt.% of polymer. With our preparation procedure, it proved possible to produce GDEs with a homogeneous microstructure and fine distribution of PTFE up to at least 40 wt.%. At higher polymer contents we observed the formation of agglomerates of PTFE in the catalyst layer as can for example be seen in Fig. 6d showing a detail of the microstructure of an electrode containing 50% PTFE. From our standard fuel cell characterization (T = 160 °C, H_2/air, ambient pressure), we were unable to detect any important differences between the polarization curves measured with the samples containing 20 and 40% PTFE, respectively, in either of the GDEs as both MEAs had cell voltages slightly higher than 600 mV at j = 200 mA cm^{-2} and because ~250 mW cm^{-2} was obtained as the maximum power density for both samples (Fig. 7). The MEA with 60% PTFE performed significantly less satisfactorily. This might be attributed to a partial encapsulation of catalyst particles by the high volume fraction of PTFE or by the formation of non-active parts of the cell area due to large agglomerates of inert PTFE. For all subsequent studies, we chose to use GDEs with a fairly high binder content of 40% PTFE, which is close to the value predicted to be optimal for PEFC catalyst layers with Nafion and PTFE as binders [31].

3.4.3. Introduction of ABPBI into the catalyst layer

We investigated different ways of introducing ABPBI into the catalyst layers because it could at least partially replace PTFE as binder and might additionally prevent leaching of the electrolyte from the MEA during fuel cell operation due to its affinity for phosphoric acid. One approach consisted of precipitating ABPBI on the catalyst support by dripping a dispersion of 20% Pt/C in a solution of (not cross-linked) ABPBI into an excess of a non-solvent such as water or terpineol with vigorous stirring. After washing and filtrating the powder, it was used for the standard preparation of catalyst inks. Alternatively previously prepared GDEs were loaded with ABPBI by spraying a solution of the polymer on top of the catalyst layer or by dipping it into the ABPBI solution. A one-step procedure for the preparation of the catalyst layer by directly adding an ABPBI solution to a dispersion of the catalyst (and if applicable PTFE) in for example DMAc or a mixture of formic and phosphoric acid (cf. [6,12,13,17,21,32]) under prolonged ultrasonication has not been studied yet. Although different authors have explicitly claimed the introduction of polybenzimidazole to be advantageous for fuel cell performance [21,33–35], this was not achieved under the experimental conditions of this study. In all cases, ABPBI amounts as low as 2 wt.% led to a significant decrease of fuel cell performance. As we observed very low gas permeabilities of the ABPBI-containing GDEs (by measuring the respective Gurley numbers, results not

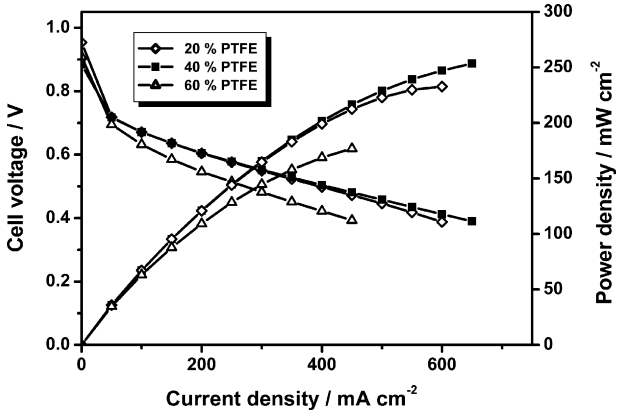

Fig. 7. Cell performance of ABPBI-based MEAs with different amounts of PTFE in the 20% Pt/C-based catalyst layer (~1.0 mg Pt cm^{-2} and 20 mg H_3PO_4 cm^{-2} per electrode).

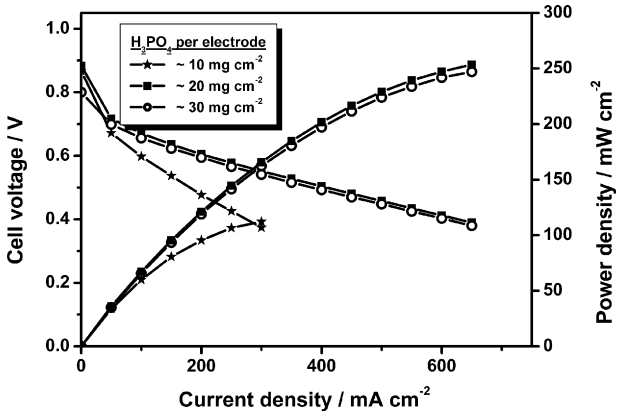

Fig. 8. Influence of the amount of acid impregnation of the catalyst layers of GDEs (20% Pt/C, 40% PTFE) on the performance of MEAs after assembling these GDEs with undoped ABPBI membranes.

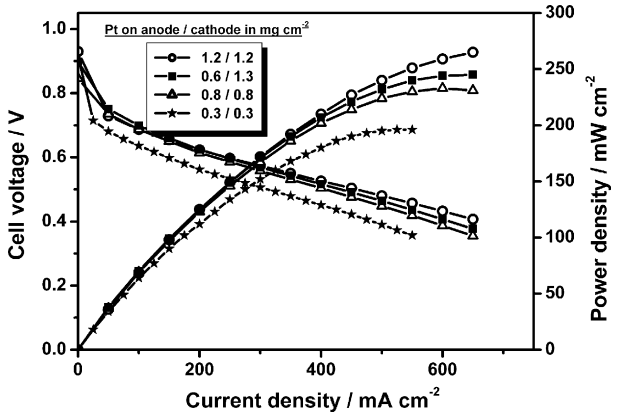

Fig. 9. Comparison of the polarization curves for MEAs with GDEs of the same composition (20% Pt/C, 40% PTFE, 20 mg H_3PO_4 cm^{-2} per electrode) but different catalyst loadings.

shown here) and supported by the observation that MEAs prepared from these electrodes needed rather high gas flows (up to $\lambda = 6$) to work reasonably well, we attribute this to the strong film-forming properties of our ABPBI solution.

3.4.4. On the amount of acid impregnation of GDEs

An acid impregnation of about 6 mg H_3PO_4 cm^{-2} per electrode would be sufficient for maximum conductivity of the membrane if the complete amount of phosphoric acid was transferred from the catalyst layers to the membrane during the first heating of the MEA (cf. Section 3.4.1). Some additional phosphoric acid is assumed to be necessary for good proton conductivity within the GDEs. Loading both electrodes based on 20% Pt/C (about 150 μm thick) with 10 mg H_3PO_4 cm^{-2} was not sufficient to achieve good fuel cell performance as this MEA only delivered 110 mW cm^{-2} as the peak power density (Fig. 8). Only with a much higher excess of phosphoric acid, such as 20 or 30 mg cm^{-2} per electrode, was good cell performance achieved with a maximum power density above 250 mW cm^{-2}. An even higher amount of phosphoric acid is thought to be disadvantageous as most of the pores of the catalyst layer will become filled with liquid, which is believed to be detrimental for the mass transport of the reactants. Detailed studies about the distribution of the phosphoric acid within the MEA are under way and the results will be published in a separate paper.

3.4.5. Catalyst loading

High-temperature PEM fuel cells with phosphoric acid electrolyte require relatively high catalyst loadings compared to 'classical' PEFCs with a perfluorosulfonic-acid-type membrane (e.g. Nafion®) operating at 60–90 °C. This has been attributed to anion adsorption on platinum as well as to low solubility of oxygen in and its slow diffusion through phosphoric acid within the cathodic catalyst layer [10,36–38]. In accordance with data from the open literature, we found a platinum loading of about 1 mg cm^{-2} per electrode to be a good choice. While there were no significant differences in the cell performances at technically relevant cell voltages of 500–600 mV of MEAs with platinum loadings between 0.6 and 1.2 mg cm^{-2}, an MEA with a loading of 0.3 mg cm^{-2} (which would still be reasonably high for a 'classical' PEFC) performed much less satisfactorily (Fig. 9). We observed that MEAs with a catalyst loading of 0.6–0.8 mg cm^{-2} needed more time after the break-in period and the recording of several polarization curves to reach their maximum performance, while those with loadings above 1.0 mg cm^{-2} displayed their highest power output immediately after the break-in (not detailed here). As all GDEs tested in this context were impregnated with 20 mg cm^{-2} H_3PO_4 to assure good conductivity of the membrane in the working cell, an increasing blocking of catalyst sites and of gas diffusion pathways by phosphoric acid with reduced catalyst loading (= reduced thickness of the catalyst layer) is assumed to be at least partly responsible for the relatively low performance of the MEA with the smallest catalyst loading.

3.4.6. Cell compression

The influence of the cell compression (defined by the thickness to which the MEA has been compressed in the cell relative to the sum of the thicknesses of its individual components) was only varied between 60 and 85% during this study. Within this range no significant influence of the cell compression on the fuel cell performance at 160 °C and $\lambda_{A/C} = 2/2$ was observed. This might be due to the fact that a thick and very porous gas diffusion layer was used, which can buffer these small to modest variations in compression. Accordingly, there were only very small variations in the cell resistances if at all. The measured values of 120–150 mΩ cm^2 indicate an intimate bonding between the GDEs and the membrane as well as good proton conductivity within the MEA.

3.4.7. Influence of stoichiometric excesses of the reactants

An increase of the gas flows from $\lambda_{A/C} = 2/2$ to 3/3 or 6/6 led to a small increase of the cell performance in the technically relevant region of the polarization curves at cell voltages above 0.5 V (Fig. 10). While a decrease of the anodic lambda to 1.2 (and maintaining $\lambda_C = 2.0$) was possible without large performance losses, the

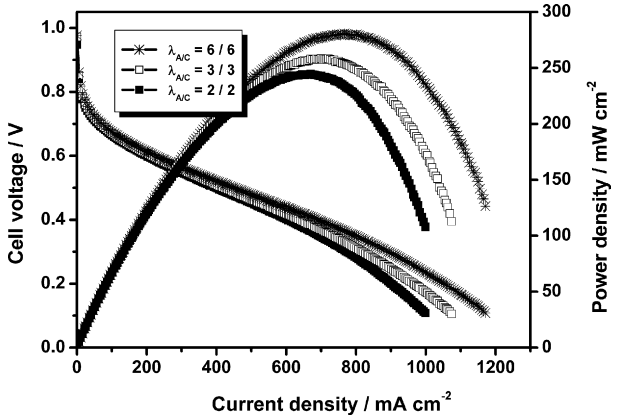

Fig. 10. Influence of the stoichiometric excess of the reactants on the fuel cell performance of an MEA (GDEs: 20% Pt/C with 1.2 mg Pt cm^{-2}, 40% PTFE, 20 mg H_3PO_4 cm^{-2} per electrode) at 160 °C using hydrogen and dry air without pressurization as the reactants.

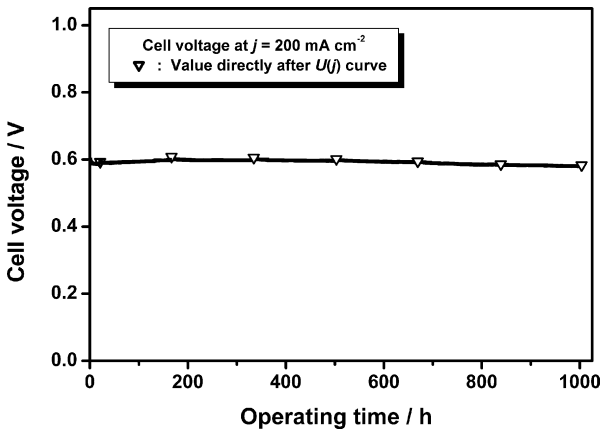

Fig. 11. Cell voltage of an MEA prepared from acid-impregnated GDEs (20% Pt/C with 1.2 mg Pt cm^{-2}, 40% PTFE, 20 mg H_3PO_4 cm^{-2} per electrode) and an undoped ABPBI membrane when the current density was fixed to $j = 200$ mA cm^{-2} during a 1000 h durability test at 160 °C (H_2/air, (both dry), ambient pressure, $\lambda_{A/C} = 2/2$, $A = 14.4$ cm^2). The first data point after the weekly recording of two polarization curves is marked by a triangle.

reduction of the cathodic gas flow ($\lambda_{A/C} = 2.0/1.2$) resulted in a 30% decrease of the current density at $U = 550$ mV (not shown here).

3.4.8. Durability

MEAs have already demonstrated good durability not only in single cells [23] but also in a first 100 W stack [22]. While the average degradation rate of an MEA (20% Pt/C with 1.2 mg Pt cm^{-2}, 40% PTFE, 20 mg H_3PO_4 cm^{-2} per electrode) during a 1000 h test under nearly steady-state conditions at 160 °C was as low as -25 μV h^{-1} (Fig. 11), dynamic load changes and start-stop cycling generally led to somewhat higher degradation rates [8,23]. For some PBI-MEAs even better long-term stability of cell performance has been reported [8,11,39]. We identified the loss of catalytically active sites by an increasing mean particle size in the electrodes, especially in the cathode, as the main cause of these performance losses ([23], for comparison see also [40]). Indeed, the mean diameter of platinum crystallites (deduced from X-ray powder diffractograms) increased from 2.5 nm in fresh GDEs to 5.2 in the anodic and to 6.5 nm in the cathodic catalyst layer after the 1000 h test under nearly steady-state conditions [23]. Leaching of phosphoric acid from the MEA during cell operation clearly plays a minor role under these experimental conditions [8,23].

4. Conclusions and outlook

We have established a novel (or long-neglected [24]) technique for the introduction of phosphoric acid into high-temperature PEFCs by impregnating thick catalyst layers – deposited on a dense microporous layer (serving as an effective barrier layer against leaching of H_3PO_4 from the MEA) of a GDL – with phosphoric acid and assembling these as both anodes and cathodes with an undoped ABPBI membrane. Redistribution of the electrolyte was found to be a quick process as such MEAs deliver high current densities immediately after start-up. So far, the best cell performance has been obtained using GDEs with a platinum loading amounting to ~1.0 mg cm^{-2} based on 20% Pt/C as catalyst and containing 40% PTFE as a binder when these active layers have been impregnated with 20 mg H_3PO_4 cm^{-2}. With hydrogen and dry air as reactants at ambient pressure and moderate gas flows, power densities of around 250 mW cm^{-2} have been obtained at 160 °C. MEAs prepared in this way displayed good durability during a 1000 h test with an average degradation rate of only -25 μV h^{-1} during nearly steady-state operation at 160 °C. Further developments will concentrate on the use of ABPBI membranes with an acid uptake capability even exceeding the present 3.1 moles of H_3PO_4 per repeat unit of ABPBI (specific conductivity of 80 mS cm^{-1} at 140 °C in quasi-dry air) as well as on redesigning the cathodic catalyst layer. Studies elucidating the acid distribution in this type of MEA are underway. We believe our easy and very reproducible MEA preparation technique can be used with any type of high-temperature PEFC with a phosphoric acid/benzimidazole type electrolyte system and that it is especially beneficial for the fabrication of MEAs for stacks with a large area of the individual cells as only mechanically robust materials have to be handled while assembling the MEA.

Acknowledgements

This work would not have been possible without Sina Chirayath's experience in and good intuition for the design and manufacture of catalyst layers for PEFCs. We would like to thank Irene Konradi for carrying out the water and acid uptake experiments, Egbert Wessel at Forschungszentrum Jülich's IEF-2 for the SEM images, as well as Birgit Kohnen and Hans-Friedrich Oetjen for performing the fuel cell tests.

This work was part of a joint project with FuMA-Tech GmbH funded by the German Federal Ministry of Economics and Technology under contract number 0326878A.

References

[1] J. Divisek, H.-F. Oetjen, V. Peinecke, V.M. Schmidt, U. Stimming, Electrochim. Acta 43 (1998) 3811–3815.
[2] J. Vogel, Paper Presented at the DOE Hydrogen Program 2008 Annual Merit Review, Arlington, Virginia, USA, 2008.
[3] J.S. Wainright, J.-T. Wang, D. Weng, R.F. Savinell, M. Litt, J. Electrochem. Soc. 142 (1995) L121–L123.
[4] Y.-L. Ma, J.S. Wainright, M.H. Litt, R.F. Savinell, J. Electrochem. Soc. 151 (2004) A8–A16.
[5] Q. Li, R. He, J.O. Jensen, N.J. Bjerrum, Fuel Cells 4 (2004) 147–159.
[6] C. Pan, Q. Li, J.O. Jensen, R. He, L.N. Cleemann, M.S. Nilsson, N.J. Bjerrum, Q. Zeng, J. Power Sources 172 (2007) 278–286.
[7] B.C. Benicewicz, S. Yu, L. Xiao, K. Perry, Paper Presented at Fuel Cells 2007 – Advances in Materials for Proton Exchange Membrane Fuel Cell Systems, American Chemical Society – Polymer Division, Asilomar, California, USA, 2007.
[8] S. Yu, L. Xiao, B.C. Benicewicz, Fuel Cells 8 (2008) 165–174.
[9] G. Calundann, Paper Presented at 2006 Fuel Cell Seminar, Honolulu, Hawaii, USA, November 13–17, 2006.
[10] T.J. Schmidt, J. Baurmeister, J. Power Sources 176 (2008) 428–434.
[11] K. Foli, O. Gronwald, S. Haufe, S. Kiel, U. Mähr, D. Melzner, A. Reiche, F. Walter, S. Weisshaar, Paper Presented at 2006 Fuel Cell Seminar, Honolulu, Hawaii, USA, November 13–17, 2006.
[12] J. Lobato, P. Canizares, M.A. Rodrigo, J.J. Linares, J.A. Aguilar, J. Membr. Sci. 306 (2007) 47–55.
[13] K. Scott, S. Pilditch, M. Mamlouk, J. Appl. Electrochem. 37 (2007) 1245–1259.
[14] S.J. Lee, J.Y. Shin, T.W. Song, J. Peng, Paper Presented at the 211th ECS Meeting, Abstract #0394, Chicago, Illinois, USA, May 5–10, 2007.
[15] T.-H. Kim, T.-W. Lim, J.-C. Lee, J. Power Sources 172 (2007) 172–179.
[16] N. Gourdoupi, K. Papadimitriou, S. Neophytides, J.K. Kallitsis, Fuel Cells 8 (2008) 200–208.
[17] (a) J. Kerres, F. Schönberger, A. Chromik, T. Häring, Q. Li, J.O. Jensen, C. Pan, P. Noye, N.J. Bjerrum, Fuel Cells 8 (2008) 175–187;
(b) Q. Li, J.O. Jensen, C. Pan, V. Bandur, M.S. Nilsson, F. Schönberger, A. Chromik, M. Hein, T. Häring, J. Kerres, N.J. Bjerrum, Fuel Cells 8 (2008) 188–199.
[18] H.-J. Kim, S.Y. Cho, S.J. An, Y.C. Eun, J.-Y. Kim, H.-K. Yoon, H.-J. Kweon, K.H. Yew, Macromol. Rapid Commun. 25 (2004) 894–897.
[19] J.A. Asensio, P. Gomez-Romero, Fuel Cells 5 (2005) 336–343.
[20] P. Krishnan, J.-S. Park, C.-S. Kim, J. Power Sources 159 (2006) 817–823.
[21] J.-H. Kim, H.-J. Kim, T.-H. Lim, H.-I. Lee, J. Power Sources 170 (2007) 275–280.
[22] C. Wannek, H. Dohle, J. Mergel, D. Stolten, ECS Trans. 12 (2008) 29–39.
[23] C. Wannek, B. Kohnen, H.-F. Oetjen, H. Lippert, J. Mergel, Fuel Cells 8 (2008) 87–95.
[24] J.-T. Wang, R.F. Savinell, J. Wainright, M. Litt, H. Yu, Electrochim. Acta 41 (1996) 193–197.
[25] D. Melzner, A. Reiche, U. Mähr, S. Kiel, German Patent Application DE 10301810 A1, filed on January 20, 2003.
[26] C. Jacksch, W. Zipprich, G. Hübner, German Patent Application DE 102004024845 A1, filed on May 13, 2004.
[27] C. Wannek, S. Chirayath, I. Konradi, J. Mergel, W. Lehnert, Paper Presented at Progress MEA 2008 – 1st International Carisma Conference, La Grande Motte, France, September 21–24, 2008.
[28] M. Schuster, FuMA-Tech GmbH, personal communication.

[29] T.C. Gruber, T.W. Zerda, M. Gerspacher, Carbon 31 (1993) 1290.
[30] J. Xie, K.L. More, T.A. Zawodzinski, W.H. Smith, J. Electrochem. Soc. 151 (2004) A1841.
[31] E. Antolini, L. Giorgi, A. Pozio, E. Passalacqua, J. Power Sources 77 (1999) 136–142.
[32] J. Lobato, M.A. Rodrigo, J.J. Linares, K. Scott, J. Power Sources 157 (2006) 284–292.
[33] S. Haufe, U. Mähr, S. Kiel, D. Melzner, A. Reiche, German Patent Application DE 102004032999 A1, filed on July 8, 2004.
[34] J. Belack, I. Kundler, T. Schmidt, O. Uensal, J. Kiefer, C. Padberg, M. Weber, International Patent Application WO 2005/023914 A2, filed on September 4, 2004.
[35] C. Jacksch, G. Hübner, German Patent Application DE 102004063457 A1, filed on December 23, 2004.
[36] F. ElKadiri, R. Faure, R. Durand, J. Electroanal. Chem. 301 (1991) 177–188.
[37] F. Gan, D.-T. Chin, J. Appl. Electrochem. 23 (1993) 452–455.
[38] Z. Liu, J.S. Wainright, M.H. Litt, R.F. Savinell, Electrochim. Acta 51 (2006) 3914–3923.
[39] Q. Li, P. Noye, J.O. Jensen, C. Pan, N.J. Bjerrum, Abstract to the 210th ECS Meeting, Cancun, Mexico, October 29–November 3, 2006.
[40] J. Hu, H. Zhang, Y. Zhai, G. Liu, J. Hu, B. Yi, Electrochim. Acta 52 (2006) 394–401.